Journal of Molecular Structure 1032 (2013) 48–55

Contents lists available at SciVerse ScienceDirect

Journal of Molecular Structure

journal homepage: www.elsevier.com/locate/molstruc

Thiosaccharine disulfide: Synthesis, crystal structure, spectroscopic characterization and theoretical study

Ricardo M. Ferullo [a], Alejandro Granados [b], Anabel Lanterna [b], Jorge A. Güida [c,d], Oscar E. Piro [e], Eduardo E. Castellano [f], Mariana Dennehy [a,*]

[a] INQUISUR (CONICET), Departamento de Química, Universidad Nacional del Sur, Avda. Alem 1253, B8000CPB, Bahía Blanca, Argentina
[b] INFIQC (CONICET), Departamento de Química Orgánica, Universidad Nacional de Córdoba, CP 5000, Córdoba, Argentina
[c] CEQUINOR, Facultad de Ciencias Exactas y Facultad de Ingeniería, Universidad Nacional de La Plata, CC 962, 1900 La Plata, Argentina
[d] Departamento de Ciencias Básicas, Universidad Nacional de Luján, Rutas 5 y 7, Luján, Argentina
[e] Departamento de Física and Instituto IFLP (CONICET CCT-La Plata), Facultad de Ciencias Exactas, Universidad Nacional de La Plata, CC 67, 1900 La Plata, Argentina
[f] Instituto de Física de São Carlos, Universidade de São Paulo, CP 369, 13560 São Carlos, SP, Brazil

HIGHLIGHTS

- The thiosaccharine disulfide was synthesized.
- X-ray study indicates that the disulfide shows an equatorial conformation.
- ^{1}H, ^{31}P and ^{13}C NMR, IR and UV–Visible spectroscopy studies confirmed the structure.
- Thiosaccharine disulfide cannot be reduced to the initial thiols in solution.
- Theoretical calculations are a good representation of the compound.

ARTICLE INFO

Article history:
Received 15 April 2012
Received in revised form 12 June 2012
Accepted 24 July 2012
Available online 7 August 2012

Dedicated to the memory of Prof. Dr. Oscar V. Quinzani

Keywords:
Thiosaccharine
Disulfide
Crystal structure
Infrared
Raman
UV–Visible spectroscopy

ABSTRACT

The title compound, (thiosaccharine disulfide), bis[1,1′dioxide-2,3-dihidro-1,2-benzoisothiazol]disulfide, $(tsac)_2$ has been synthesized and fully characterized by UV–Visible, IR, Raman, ^{1}H and ^{13}C NMR spectroscopy elemental analysis and structural X-ray crystallography. A DFT theoretical study has been performed and good agreement between experimental and theoretical values of structural parameters and vibration frequencies have been achieved.

1. Introduction

Thiols are compounds chemically capable to bind to metals, especially to heavy metals. They have also reducing character of both metal ions and other species. The chemical oxidation of the thiols usually leads to the corresponding organic disulfides [1–4]. The study of organic disulfides is of continuous interest, because it is related to the redox behavior of proteins in natural systems containing the cysteine amino-acid which can be oxidized with the concomitant disulfide production [3,5–7]. Oxidation of cysteine's sulfhydryl group (–SH) forms variously sulfenic (–SOH), sulfinic ($–SO_2H$), and sulfonic/cysteic ($–SO_3H$) acids, inter-chain/intra-chain disulfide bridges (–S–S–), or thiolsulfinates.

A number of important studies on saccharin (1,2-benzisothiazol-3-(2H)-one-1,1,-dioxide), one of most widely used artificial sweetening agents, and on its metal complexes have been performed during the last few years, mainly because of its suspected cancerogenic nature [8]. However, there is less information concerning thiosaccharine, (1,2-benzoisothiazol-3-(2H)-thione-

* Corresponding author. Tel.: +54 291 4595101x3592; fax: +54 291 4595160.
E-mail address: mdennehy@uns.edu.ar (M. Dennehy).

0022-2860/$ - see front matter © 2012 Elsevier B.V. All rights reserved.
http://dx.doi.org/10.1016/j.molstruc.2012.07.043

1,1-dioxide), $\{C_6H_4S(O_2)NC\}S\text{-}S\{CNS(O_2)C_6H_4\}$, the thione form of saccharin. Thiosaccharine is an electron-rich and poly-functional ligand with the ability to coordinate to metal centers in many different ways. Some ionic thiosaccharinates and metal thiosaccharinato complexes (with Cd(II), Hg(II), Tl(I), Pb(II), Bi(III) Ag(I), Pd(II), Cu(I) and Au(I)) have been systematically characterized to date [9,10], and only the biological activity of bismuth(III) thiosaccharinate complexes against helicobacter pylori has been recently reported [9s].

As it is well-known for other heterocyclic thiones, thiosaccharine has in solution a tautomeric equilibrium between the thiol and the thione forms. When the thiosaccharine is oxidized, through the action of metals or of conventional chemical agents, the thiol form produces the corresponding disulfide (Scheme 1).

We present here a structural and spectroscopic study of the thiosaccharine disulfide. Further insight into the molecular structure was provided by theoretical calculations using the DFT approach.

2. Experimental section

2.1. General remarks

All chemicals were of analytical reagent grade and used as purchased. Solid thiosaccharine (Htsac) in its α-form was prepared following the technique published by Schibye et al. [11] and characterized by melting point and IR spectroscopy analysis. The IR spectra of the substances as KBr pellets and Nujol mulls were recorded in the 4000–400 cm^{-1} range on a Nicolet Nexus FTIR spectrometer. The Raman spectra of the solids, in the region between 3500 and 100 cm^{-1}, were obtained with a FRA 106 accessory mounted in a Bruker IFS 66 FTIR instrument, using the 1064 nm excitation line from an Nd–YAG laser. The UV–Visible spectra of the solutions were performed with a Shimadzu UV-1800 spectrophotometer. ^1H and ^{13}C spectra of the substances solutions were collected on a Bruker Avance II NMR 400 MHz instrument (at 400 and 100 MHz, respectively). Experiments were performed in deuterated dimethylsulfoxide, DMSO-d_6 and in deuterated chloroform, $CDCl_3$; using as internal reference the residual peak of solvent and tetramethylsilane, respectively. Irradiation experiments were performed with white light from an energy saving lamp of 11 W at 20 cm away.

2.2. Synthesis of the disulfide

The disulfide was prepared oxidizing 10 mL of an aqueous solution of thiosaccharine (Htsac) (200 mg in 40 mL) with 3 mL of a $KMnO_4$ aqueous solution, in molar ratio 5:1. The obtained solid was separated by filtration and washed with water. Yield: 75%.

The same product was obtained using H_2O_2 or HNO_3. It was also obtained as a by-product of the synthesis of the Cu(I) thiosaccharinate and Au(I) thiosaccharinate (when the starting reactants were Cu(II) [9e] or Au(III) [10]).

Crystals suitable for structural X-ray diffraction studies were obtained through re-crystallization of the crude yellowish solid in CH_2Cl_2 by slow evaporation of the solvent.

ESI–HRMS: *m/z* calcd for $C_{14}H_8N_2O_4S_4$ 395.93669; found 418.92442 $[M + Na]^+$ Analytical percent composition calculated for $C_{14}H_8N_2O_4S_4$: C, 42.4; H, 2.0; and N, 7.1%. Found: C, 41.8; H, 1.9; and N, 7.2%.

2.3. X-ray crystallography

The X-ray measurements were performed on an Enraf–Nonius Kappa-CCD diffractometer with graphite-monochromated Mo Kα (λ = 0.71073 Å) radiation. Diffraction data were collected (φ and ω scans with κ-offsets) with COLLECT [12]. Integration, scaling and reduction of the diffraction intensities were performed with HKL DENZO–SCALEPACK [13] suite of programs. The data were corrected empirically for absorption effects [14]. The unit cell parameters were obtained by least-squares refinement based on the angular settings for all collected reflections using HKL DENZO–SCALEPACK. The structure was solved by direct methods with SHELXS-97 [15] and the molecular model refined by full-matrix least-squares procedure on F^2 with SHELXL-97 [16]. The H-atoms were positioned stereo-chemically and refined with the riding model. Crystal data and refinement results for $(tsac)_2$ are summarized in Table 1.

2.4. Theoretical calculations

Density Functional Theory (DFT) quantum–mechanical calculations were done in order to optimize the geometry of the disulfide. The gradient-corrected Becke's three parameters hybrid exchange function in combination with the correlation function of Lee, Yang and Parr (B3LYP) as implemented in the software package Gaussian09 [17] was used. Geometry optimization procedures were started from the experimental crystallographic data of $(tsac)_2$ employing the 6-31G** basis sets. The atomic charges were computed according to the NBO (Natural Bond Orbital) population analysis which is based on quantum perturbation theory [18].

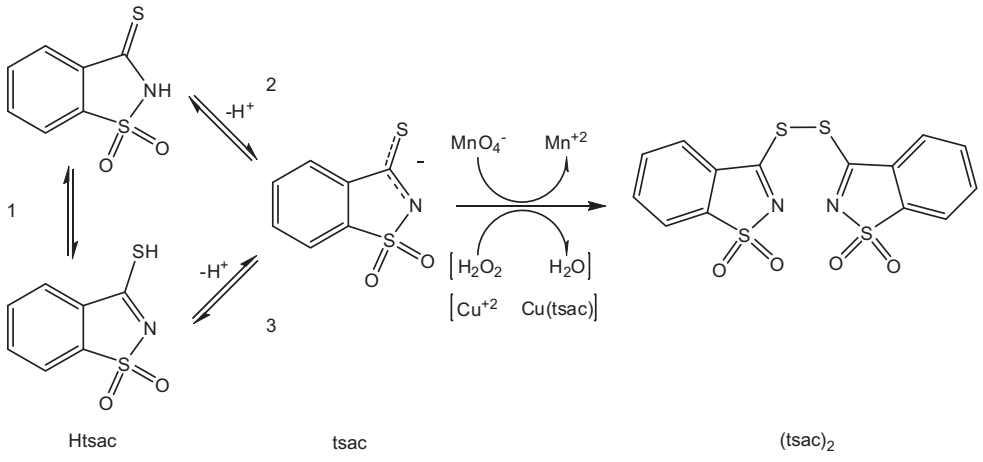

Scheme 1. Disulfide synthesis.

Table 1
Crystal data and structure refinement results for $(tsac)_2$.

Empirical formula	$C_{14}H_8N_2O_4S_4$
Formula weight	396.46
Temperature	293(2) K
Wavelength	0.71073 Å
Crystal system	Monoclinic
Space group	$P2_1/n$
Unit cell dimensions	a = 11.545(1) Å
	b = 10.562(1) Å
	c = 12.343(1) Å
	β = 96.56(1)°
Volume	1495.2(2) Å^3
Z	4
Density (calculated)	1.761 Mg/m^3
Absorption coefficient	0.659 mm^{-1}
F(000)	808
Crystal size	0.355 × 0.275 × 0.192 mm^3
Theta range for data collection	2.29–26.00°.
Index ranges	$-14 \leqslant h \leqslant 14$, $-13 \leqslant k \leqslant 13$, $-15 \leqslant l \leqslant 15$
Reflections collected	12102
Independent reflections	2913 [R(int) = 0.0395]
Observed reflections [$I > 2\sigma(I)$]	2697
Completeness to theta = 26.00°	99.4%
Absorption correction	Semi-empirical from equivalents
Max. and min. transmission	0.881 and 0.790
Refinement method	Full-matrix least-squares on F^2
Data/restraints/parameters	2913/0/217
Goodness-of-fit on F^2	1.041
Final R indices[a] [$I > 2\sigma(I)$]	R_1 = 0.0270, wR_2 = 0.0715
R indices (all data)	R_1 = 0.0301, wR_2 = 0.0732
Largest diff. peak and hole	0.335 and −0.473 e.Å^{-3}

[a] R indices defined as: $R_1 = \Sigma||Fo|-|Fc||/\Sigma|Fo|$, $wR_2 = [\Sigma w(Fo^2-Fc^2)^2/\Sigma w(Fo^2)^2]^{1/2}$.

3. Results and discussion

3.1. Crystal structure

Fig. 1 shows ORTEP [19] diagrams of the molecule. Selected bond distances and angles of the $(tsac)_2$ are given in Supplementary Information (Table S1).

The isoindolic subunits are essentially planar (*rms* deviation of atoms within each subunit from its corresponding least-squares plane less than 0.058 Å), with the exception of the oxygen atoms of the SO_2 groups, with the planes subtending a dihedral angle of 66.97(2)° from each other. This value is rather low compared with other aromatic disulfides [20], as can be observed from the comparative data shown in Supplementary Information (Table S2). The S–S bond distance (2.042 Å) and the C11–S11–S21 and C21–S21–S11 angles (102.5° and 100.9°, respectively) correspond to an equatorial disulfide. Following the Shefter definition [21], a disulfide is define as *equatorial* when the dihedral angle between the aromatic ring and the disulfide bridge (S–S–C–X) is near 0°

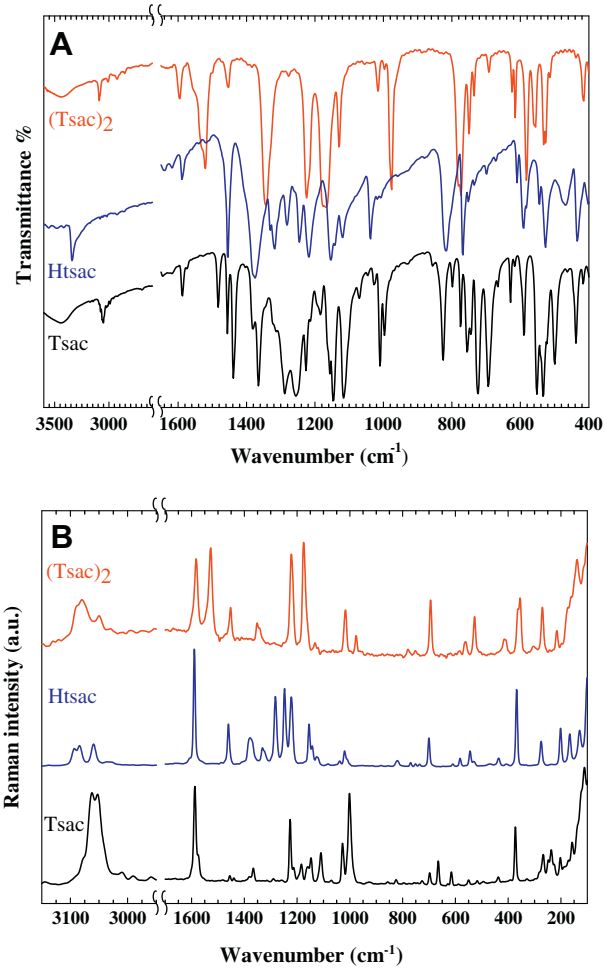

Fig. 2. (a) Infrared and (b) Raman spectra of $(tsac)_2$, Htsac and tsac.

(see Table S1). When the mentioned angle is open, ideally 90°, the disulfide is classified as *axial*.

The Si1–Ci1 (i = 1, 2) bond distances (average 1.750 Å) correspond to single bonds while Ci1–Ni bonds (average 1.287 Å) are essentially of double bound character.

3.2. FT-IR, Raman and UV–Visible spectra

The vibrational spectra of the disulfide are consistent with the X-ray structure. The infrared absorption and Raman dispersion spectra are shown in Fig. 2. A selection of the characteristic bands

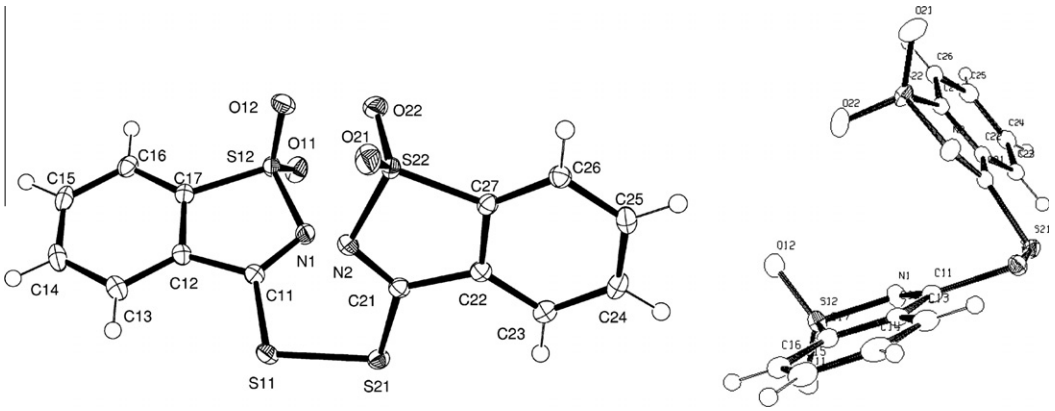

Fig. 1. Molecular diagram of two different views of $(tsac)_2$ showing the labeling of the non-H atoms and their displacement ellipsoids at 50% probability level.

and calculated frequencies and their assignments are presented in Table 2.

The most interesting bands of $(tsac)_2$ are those related to the five-member ring, located between 1500 and 400 cm^{-1}, and the low-energy sulfur–sulfur vibration, located at 515 cm^{-1}. A similar ν(S–S) frequency (471 cm^{-1}) was observed in N,N,N′,N′-tetramethylformamidinium disulfide at 471 cm^{-1} [22]. The thione benzene ring vibrations of $(tsac)_2$ show no significant differences compared with the thione benzenic ring vibrations of Htsac or PNP(tsac) (bis(triphenylphosphine)-iminium thiosaccharinate) [23]. The bands attributable to the N–H bond vibrations, namely ν(NH) and δ(NH) modes, which in the thiosaccharine molecule appear at 3341 and 1376 cm^{-1}, respectively, are absent in the spectra of the disulfide. There are also no bands between 3000 and 2550 cm^{-1} (the ν(SH) absorption region). The stretching motion of the reinforced C–N (1521 cm^{-1}) bonds bands appear at higher wave numbers compared to the values found for the "free" thiosaccharinate in PNPtsac, while those due to the stretching of the weakened C–S (977 cm^{-1}) bonds move to lower frequencies (for PNP(tsac) ν(CN):1365, and $\nu(CS_{exo})$:1010 cm^{-1}) (see Supplementary information Table S3).

These frequency shifts reflect the changes in the bond orders of the thioamidate functional groups upon re-localization of the negative charge.

The UV–Visible spectrum of the disulfide was registered in $CHCl_3$ solution. The spectrum of the disulfide solution in $CHCl_3$ shows an intense broad band at 271 nm (see Supplementary Information (Figure S1)). The shoulders at 346 and 354 nm, respectively are due to the $\pi \rightarrow \pi^*$ transitions of the $C–S_{exo}$ thiocarbonilic bond.

3.3. ^1H and ^{13}C NMR spectra

To further characterize $(tsac)_2$, we measured its ^1H and ^{13}C NMR spectra and compared them with the corresponding ones

Table 2
Experimental and theoretical vibration frequencies (cm^{-1}) and mode assignments of $(tsac)_2$.

Assignment[a]	A symmetry vibrations[b]						B symmetry vibrations[b]					
	IR[c]		Raman[c]		Calculated[d]		IR[c]		Raman[c]		Calculated[d]	
ν(CH)					3223	0					3223	14
ν(CH)					3216	3					3216	2
ν(CH)	3089	w			3206	7			3080	m	3206	34
ν(CH)					3198	1			3050	w	3198	1
ν(CC)	1595	w			1648	35					1650	22
ν(CC)	1556	sh			1632	4			1582	s	1633	1
ν(CN)	1532	sh	1528	s	1593	92	1521	m			1586	165
ν(CH)					1492	1					1492	2
ν(CH)			1452	m	1484	3	1454	w			1484	5
ν(CH)					1373	5					1373	5
$\nu_s(SO_2)$	1344	vs	1351	w	1317	197	1344	vs			1320	189
δ(CH)					1302	0					1302	0
ν(φC)			1222	s	1236	32	1226	s			1235	291
δ(CH)					1190	3					1189	13
$\nu_s(SO_2)$, δ(NSC)	1166	vs			1133	265	1176	s	1175	vs	1137	148
ν(φS),$\nu_s(SO_2)$	1130	m			1158	119			1132	vw	1158	53
δ(CH)			1017	m	1065	1	1016	m			1066	9
ν(CC)					1044	2					1044	3
δ(CH)					1009	0					1009	0
ν(CS), δ(CCN)			976	w	979	50	977	s			978	214
γ(CH)					967	0					967	0
γ(CH)					888	0					888	0
γ(CH)	781	sh	780	vw	777	41	781	sh	780	vw	776	47
δ(CNS), ν(NS)	774	vs			758	113					760	6
δ(CCC)					743	3	735	w			745	4
ν(NS), ν(CS)	750	m	751	vw	722	61	750	m	751	vw	723	29
δ(CCC)			694	m	698	6	6902	vw			698	14
γ(φCN), ν(CS)	624	vw			632	10	615	m			619	11
δ(CCC)	582	s			573	10			583	vw	572	49
$\delta(SO_2)$, ν(SS)	532	m			545	65	559	m	562	w	554	28
γ(CCC)					529	15					529	16
$\delta w(SO_2)$			526	m	518	0	526	m			517	46
ν(SS)	513	w	515	vw	503	7						
γ(CCC)					425	2					424	2
δ(φS), ν(CS)					406	9	416	m	412	vw	407	23
$\gamma(C_7NS)$					403	6					395	2
$\delta(C_7NS)$			362	m	333	1			354	m	333	5
γ(φSNCφ), $\gamma_r(SO_2)$			270	m	285	0					285	0
δ(isoindol)			216	w	257	1					211	6
τ(CSSC)					162	0						
γ(isoindol)			139	s	143	0					132	0
δ(φCN), ν(φS), $\delta w(SO_2)$					118	2			303	vw	293	2
τ(isoindol), δ(CSS)					101	1					102	1
ρ(isoindol), τ(CSSC)					16	0			120	w	122	1
$\rho(C_7NS)$					81	0					84	1
τ(SSCN), τ(CSSC)					17	3					14	5

[a] ν: Stretching, δ: in plane bending, γ: out of plane bending, φ: bencenic ring, as: asymmetric, s: symmetric, iso: isoindolic ring.
[b] Considering the molecule belonging to the C_2.
[c] vs: Very strong, s: strong, m: medium, w: weak, vw: very weak, sh: shoulder.
[d] Calculated using DFT theory: Basis set: 6–31G**. IR intensity (km mol^{-1}).

of Htsac. The ^{1}H and ^{13}C NMR chemical shifts (δ) of Htsac and $(tsac)_2$ in different solvents are given in Supplementary Information (Table S4). As it is known, a disulfide type pyridine or pyrimidine derivate in solution could easily be reduced to the initial thiols. The thiol, in turn, can easily be oxidized to the corresponding symmetrical disulfide. As these compounds have structures comparable to Htsac and $(tsac)_2$, we have been careful in performing all the spectra in dark conditions and data acquisitions were taken immediately after the preparation of the solutions.

To further study the $(tsac)_2$ in solution, ^{1}H NMR spectra in different solvents (DMSO-d_6, $CDCl_3$ and D_2O) were performed monitoring along several days to follow the changes when the solutions were kept in dark, or exposed to direct light in the same solvent. Analogous experiments were also performed with Htsac solutions.

When 18.8 mg of $(tsac)_2$ is added to 0.75 mL of DMSO-d_6 a milky-like suspension is obtained. The ^{1}H NMR spectrum is acquired immediately after the preparation of the suspension. Then it is found that the signal corresponding to the thiol proton (proton 1) is not observed, in agreement with the structure of the disulfide compound. After several minutes, the suspension changes in dark conditions from a milky aspect to a transparent solution and the ^{1}H NMR spectrum changes consequently. A signal at 13.42 ppm appears but, after one night keeping the sample in the in dark, this signal shifts to high field and another signal appears at 13.02 ppm. The group of signals from 7.88 to 8.27 ppm changes as well as the time goes on. The suspension alterations were followed by ^{1}H NMR as it is shown in Fig. 3. The changes occur even when the suspension is kept in different irradiated conditions (solution keeps in dark as well as when it is irradiated with white light from an energy-saving lamp of 11 W at 20 cm away).

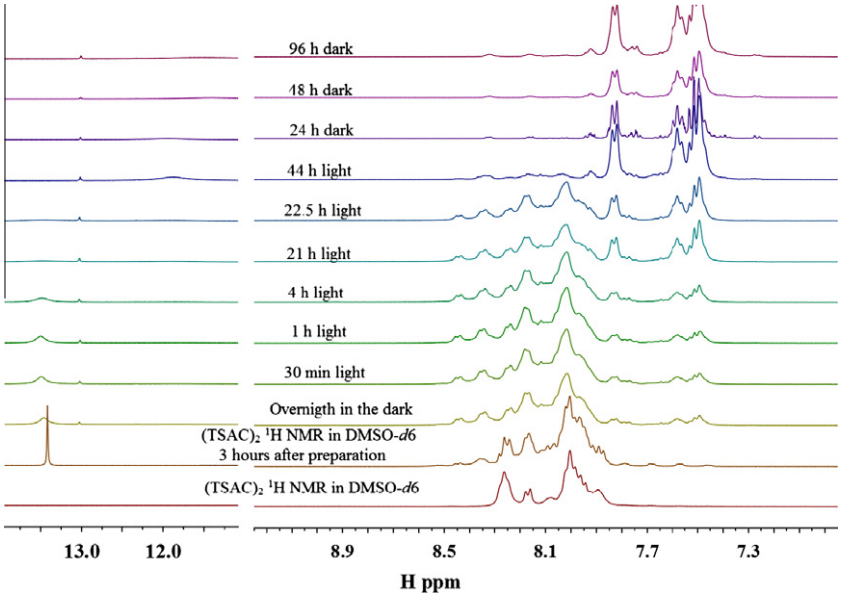

Fig. 3. ^{1}H NMR spectra of $(tsac)_2$ in DMSO-d_6 at different time and irradiation conditions.

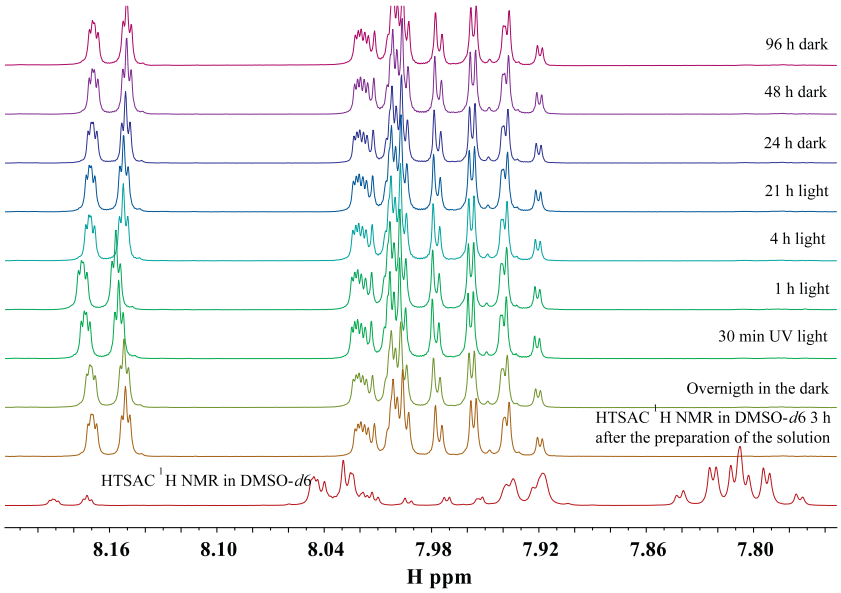

Fig. 4. ^{1}H NMR spectra of Htsac in DMSO-d_6 at different time and irradiation conditions.

All changes are irreversible and the process seems to be not the redox reaction of disulfide that should raise the ^{1}H NMR spectrum of the initial thiol (Htsac) which is not observed at all.

The solubility of $(tsac)_2$ in $CDCl_3$ is very low, and ^{1}H NMR spectra did not show any change after monitoring them with time for several days in both conditions, namely, keeping the samples in the dark or irradiating them with white light. Finally, $(tsac)_2$ solubility in D_2O is negligible and ^{1}H NMR signals are indistinguishable from noise.

On the other hand, the ^{1}H NMR spectrum was acquired when 6.6 mg of Htsac were dissolved in 0.75 mL of DMSO-d_6. ^{1}H NMR spectrum of the Htsac solution changes in dark conditions several minutes after the preparation of the solution (Fig. 4). The most important changes are the absence of the group of signals from 7.77 to 7.84 ppm, the high field shift of signals at 8.19 ppm and the complete different coupling and intensity of bands from 7.90 to 8.06. Moreover, the signal at 10.30 ppm (not shown), which could be attributed to the thiol proton (proton 1), disappears. After that, the signals persist in the ^{1}H NMR spectra even when the irradiation conditions were changed from dark to light as it is shown in Fig. 4. This could be attributed to different processes. The first one that we could mention is the aggregation of Htsac, although with the addition of HP β-CD, or even gold nanoparticles, the reversible process (disaggregation) was not achieved. Other process could be the tautomeric equilibrium between thiol and thione form, but in this case, we demonstrate that the process is not reversible even if the polarity or the temperature of the solution is changed. Finally, we could attribute the changes to a direct complexation between Htsac and the solvent molecules, which can interact by H-bond [24].

Moreover Htsac solution in $CDCl_3$ remains its ^{1}H NMR signals upon standing in dark conditions but if Htsac is exposed to direct visible light ^{1}H NMR spectra changes with time. The band at 8.20 ppm disappears at the time while a new band at 8.05 ppm comes into sight. Furthermore, the signals between 7.80 and 7.92 ppm lack their resolution and they are extended from 7.70 to 7.95 (Fig. 5). After 170 h of irradiation the sample was kept in the dark for 48 h followed by the acquisition of its ^{1}H NMR spectrum. Fig. 6 shows that the spectra are identical hence proving that the process observed under irradiation conditions is not reversible.

Finally, even when the solubility of Htsac in water is small, we followed the evolution of this compound under irradiation and also by keeping it in the dark. In both cases the compound signals remain.

3.4. DFT calculations

The structural parameters calculated for the $(tsac)_2$ are in good agreement with the experimental values. The S11–S21 and Ci1–Si1 (i = 1, 2) bond distances are overestimated. This effect has been

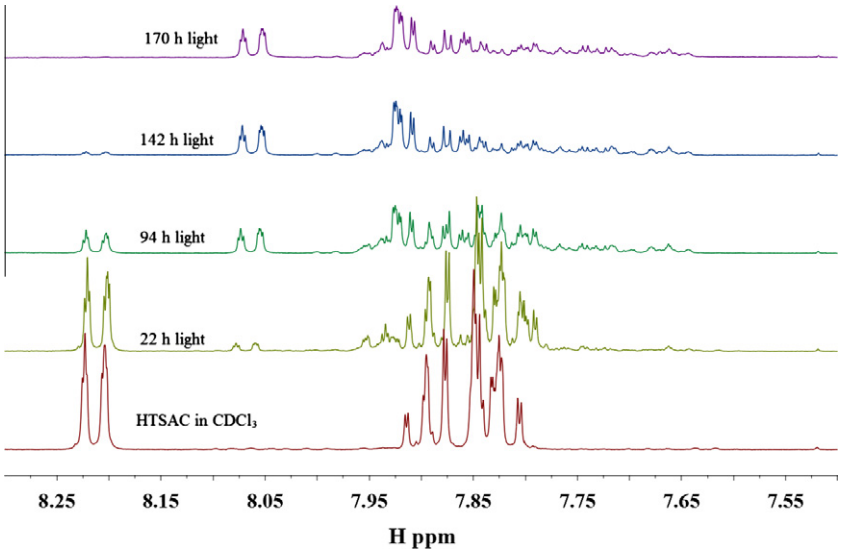

Fig. 5. ^{1}H NMR spectra of Htsac in $CDCl_3$ at different time under irradiated conditions.

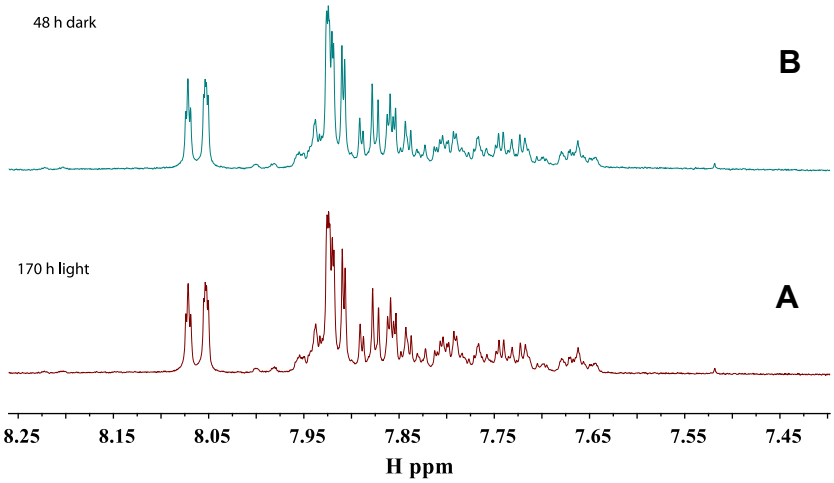

Fig. 6. ^{1}H NMR spectra of Htsac in $CDCl_3$ after 170 h under irradiated conditions (A) and subsequent 48 h kept in dark (B).

previously mentioned in theoretical predictions of other authors on other aromatic disulfides [1]. The calculated C11–S11–S21–C21 dihedral angle (85.5°) is somewhat higher than the experimental value (72.7°). This difference can be attributed to the crystal packing effects.

The calculated wave numbers corresponding to the normal vibration modes present very close values to the experimental values, though most of them overestimated in as expected for the used method [25]. However, the vibrations involving the SO_2 groups and the exocyclic Si1 ($i = 1, 2$) are very close to and even lower than the experimental values. This correlates with the differences found between calculated and observed bond distances and angles for these groups. NBO charges showed the rearrangement of the charges after the disulfide formation. Both in Htsac and in $(tsac)_2$ the carbon atoms attached with sulfur atoms are positive, whereas the remaining carbon atoms are negatively charged. The maximum atomic charges are obtained for the SO_2 oxygen atoms when compared with other atoms. Atomic charges of Htsac and of $(tsac)_2$ can be seen in Supplementary Information (Table S5).

4. Conclusions

The thiosaccharine disulfide was synthesized and fully characterized by structural X-ray diffraction and UV–Vis, IR, Raman and ^1H and ^{13}C NMR spectroscopies. The disulfide showed an equatorial conformation.

Interestingly, the structural changes generated by the oxidation process of thiosaccharine produced the corresponding frequency shifts in some infrared and Raman bands of disulfide, in agreement with the strengthening or weakening of chemical bonds, or the appearance of a new band due to the a bond formation (S–S) (see for comparison Supplementary Information Table S3). The S–S bond distance as well as the ν(S–S) infrared and Raman bands position are in agreement with data reported before for a similar bond formation in a derivate of dithiourea [22].

The theoretical calculations are a good representation of the compound.

In contrast with disulfide type pyridine or pyrimidine derivate, this thiosaccharine disulfide cannot easily be reduced to the initial thiols in solution ($CDCl_3$, DMSO-d_6 and D_2O); and the Htsac, the corresponding thiol, cannot be oxidized to the corresponding disulfide in the same conditions.

Acknowledgements

M.D and R.F. gratefully acknowledge the support of this project (Project M24/Q043) by SGCyT-UNS. Crystallographic study was supported by CONICET of Argentina and FAPESP of Brazil. O.E.P, A.L., R.F. and J.A.G. are research fellows of CONICET. The authors wish to recognize the late Dr. Oscar V. Quinzani, whose ideas and work are reflected along this paper.

Appendix A. Supplementary material

Crystallographic data for the structure has been deposited with the Cambridge Crystallographic Data Centre as supplementary data Nro CCDC 871797. Copies of the data can be obtained free of charge upon request from The Director, Cambridge Crystallographic Data Centre, 12 Union Road, Cambridge CB2 1EZ, UK. (fax: +44 1233 336033; e-mail: deposit@ccdc.cam.ac.uk; WEB: http://www.csdc.cam.ac.uk). Supplementary data associated with this article can be found, in the online version, at http://dx.doi.org/10.1016/j.molstruc.2012.07.043.

References

[1] J.D. Moreira, J.B. de Lima, D.W. Franco, Coord. Chem. Rev. 196 (2000) 197.
[2] (a) S. Stoyanov, T. Stoyanova, L. Antov, P. Karagiannidis, P.D. Akrivos, Monatsh. Chem. 127 (1996) 495;
(b) S. Stoyanov, T. Stoyanova, P. Karagiannidis, P.D. Akrivos, P. Nokolov, J. Heterocyclic Chem. 33 (1996) 927.
[3] S. Stoyanov, T. Stoyanova, P.D. Akrivos, Trends Appl. Spectros. 2 (1998) 89.
[4] R.S. Sengar, V.N. Nemikyn, P. Basu, New J. Chem. 27 (2003) 1115.
[5] W. Hu, S. Tedesco, B. McDonagh, J.A. Bárcena, C. Keane, D. Sheehan, Anal. Biochem. 398 (2010) 245.
[6] L. Zhang, C. Perry Chou, M. Moo-Young, Biotechnol. Adv. 29 (2011) 923.
[7] M. Kemp, Young-Mi Go, D.P. Jones, Free Radical Biol. Med. 44 (2008) 921.
[8] E.J. Baran, V.T. Yilmaz, Coord. Chem. Rev. 250 (2006) 1980.
[9] (a) O. Grupče, G. Jovanovski, B. Šoptrajanov, J. Mol. Struct. 267 (1992) 197;
(b) M. Penavić, G. Jovanovski, O. Grupče, Acta Crystallogr. C46 (1990) 2341;
(c) M. Penavić, O. Grupče, G. Jovanovski, Acta Crystallogr. C47 (1991) 1821;
(d) O.V. Quinzani, S. Tarulli, C. Marcos, S. Garcia Granda, E.J. Baran, Z. Anorg. Allg. Chem. 625 (1999) 1848;
(e) A. Cahil, G. Jovanovski, O. Grupče, Bull. Chem. Technol. Macedonia 19 (2000) 9;
(f) S.H. Tarulli, O.V. Quinzani, O.E. Piro, E.E. Castellano, E.J. Baran, Z. Anorg. Allg. Chem. 629 (2003) 1975;
(g) S.H. Tarulli, O.V. Quinzani, E.J. Baran, O.E. Piro, E.E. Castellano, J. Mol. Struct. 656 (2003) 161;
(h) E.J. Baran, O.E. Piro, J. Zinczuk, Z. Anorg. Allg. Chem. 632 (2006) 437;
(i) S.H. Tarulli, O.V. Quinzani, E.J. Baran, O.E. Piro, Z. Anorg. Allg. Chem. 628 (2002) 751;
(j) S.H. Tarulli, O.V. Quinzani, O.E. Piro, E.E. Castellano, E.J. Baran, J. Mol. Struct. 797 (2006) 56;
(k) M. Dennehy, O.V. Quinzani, R.A. Burrow, Acta Crystallogr. C63 (2007) m395;
(l) M. Dennehy, G.P. Tellería, S.H. Tarulli, O.V. Quinzani, S.D. Mandolesi, J.A. Guida, G.A. Echeverría, O.E. Piro, E.E. Castellano, Inorg. Chim. Acta 360 (2007) 3169;
(m) M. Dennehy, S.D. Mandolesi, O.V. Quinzani, Z. Anorg. Allg. Chem. 633 (2007) 2746;
(n) D.R. Pérez, S.H. Tarulli, O.V. Quinzani, J. Dristas, R. Faccio, L. Suescun, A.W. Mombrú, Z. Anorg. Allg. Chem. 633 (2007) 1066;
(o) M. Dennehy, O.V. Quinzani, R.M. Ferullo, S.D. Mandolesi, N. Castellani, M. Jennings, Polyhedron 27 (2008) 2243;
(p) M. Dennehy, G.P. Tellería, O.V. Quinzani, G.A. Echeverría, O.E. Piro, E.E. Castellano, Inorg. Chim. Acta. 362 (2009) 2900;
(q) M. Dennehy, O.V. Quinzani, A. Granados, R.A. Burrow, Polyhedron 29 (2010) 1344;
(r) M. Dennehy, O.V. Quinzani, S.D. Mandolesi, R.A. Burrow, J. Mol. Struct. 998 (2011) 119;
(s) P.C. Andrews, R.L. Ferrero, C.M. Forsyth, P.C. Junk, J.G. Maclellan, R.M. Peiris, Organometallics 30 (2011) 6283;
(t) M. Dennehy, E. Freire, R. Baggio, Acta Crystallogr. C68 (2012) m17;
(u) M. Dennehy, O.V. Quinzani, R. Faccio, E. Freire, Á.W. Mombrú, Acta Crystallogr. C68 (2012) m12.
[10] M. Dennehy, O.V. Quinzani, A. Granados, R.A. Burrow, Inorg. Chim. Acta 377 (2011) 77.
[11] S. Schibye, R.S. Pedersen, S.O. Lawesson, Bull. Soc. Chim. Belge. 87 (1978) 229.
[12] Enraf–Nonius. COLLECT. Nonius BV, Delft, The Netherlands, 1997–2000.
[13] Z. Otwinowski, W. Minor, in: C.W. Carter Jr, R.M. Sweet (Eds.), Methods in Enzymology, Vol. 276, Academic Press, New York, 1997, pp. 307–326.
[14] R.H. Blessing, Acta Crystallogr. Sect A. 51 (1995) 33.
[15] G.M. Sheldrick, SHELXS-97, Program for Crystal Structure Resolution, University of Göttingen: Göttingen, Germany, 1997.
[16] G. M. Sheldrick, SHELXL-97, Program for Crystal Structures Analysis. Univ. of Göttingen: Göttingen, Germany, 1997.
[17] M.J. Frisch, G.W. Trucks, H.B. Schlegel, G.E. Scuseria, M.A. Robb, J.R. Cheeseman, G. Scalmani, V. Barone, B. Mennucci, G.A. Petersson, H. Nakatsuji, M. Caricato, X. Li, H.P. Hratchian, A.F. Izmaylov, J. Bloino, G. Zheng, J.L. Sonnenberg, M. Hada, M. Ehara, K. Toyota, R. Fukuda, J. Hasegawa, M. Ishida, T. Nakajima, Y. Honda, O. Kitao, H. Nakai, T. Vreven, J.A. Montgomery, Jr., J.E. Peralta, F. Ogliaro, M. Bearpark, J.J. Heyd, E. Brothers, K.N. Kudin, V.N. Staroverov, T. Keith, R. Kobayashi, J. Normand, K. Raghavachari, A. Rendell, J.C. Burant, S.S. Iyengar, J. Tomasi, M. Cossi, N. Rega, J.M. Millam, M. Klene, J.E. Knox, J.B. Cross, V. Bakken, C. Adamo, J. Jaramillo, R. Gomperts, R.E. Stratmann, O. Yazyev, A.J. Austin, R. Cammi, C. Pomelli, J.W. Ochterski, R.L. Martin, K. Morokuma, V.G. Zakrzewski, G.A. Voth, P. Salvador, J.J. Dannenberg, S. Dapprich, A.D. Daniels, O. Farkas, J.B. Foresman, J.V. Ortiz, J. Cioslowski, D.J. Fox, Gaussian 09, Revision B.01, Gaussian, Inc., Wallingford CT, 2010.
[18] A.E. Reed, L.A. Curtiss, F. Weinhold, Chem. Rev. 88 (1988) 899.
[19] C.K. Johnson, ORTEP-II. A Fortran Thermal-Ellipsoid Plot Program. Report ORNL-5318, Oak Ridge National Laboratory, Tennessee, USA, 1976.
[20] J.A. García-Vazquez, J. Romero, A. Souza-Pedrares, M.L. Louro, A. Souza, J. Zubieta, J. Chem. Soc. Dalton Trans. (2000) 559.
[21] E. Shefter, J. Chem. Soc. B. (1970) 903.
[22] A.E. Bolzan, J.A. Güida, R.C.V. Piatti, A.J. Arvia, O.E. Piro, J.R. Sabino, E.E. Castellano, J. Mol. Struct. 871 (2007) 131.

[23] (a) M. Dennehy, O.V. Quinzani, S.D. Mandolesi, J.A. Güida, G.A. Echeverría, O.E. Piro, Monatsch. Chem. 138 (2007) 669;
(b) E.J. Baran, J. Zinczuk, J. Raman Spectros. 37 (2006) 948.
[24] A. Milani, N.A. Fadel, L. Brambilla, M. Del Zoppo, C. Castiglioni, G. Zerbi, R. Stradi, J. Raman Spectros. 40 (2009) 1110.
[25] A.P. Scott, L. Random, J. Phys. Chem. 100 (1996) 16502.